A novel *Brassica*-rhizotron system to unravel the dynamic changes in root system architecture of oilseed rape under phosphorus deficiency

Pan Yuan[1,2], Guang-Da Ding[1,2], Hong-Mei Cai[2], Ke-Mo Jin[1,2], Martin R. Broadley[3], Fang-Sen Xu[1,2] and Lei Shi[1,2*]

[1]National Key Lab of Crop Genetic Improvement, Huazhong Agricultural University, Wuhan 430070, PR China, [2]Key Lab of Cultivated Land Conservation, Ministry of Agriculture/ Microelement Research Centre, Huazhong Agricultural University, Wuhan 430070, PR China, [3]Plant and Crop Sciences Division, School of Biosciences, University of Nottingham, Sutton Bonington Campus, Loughborough LE12 5RD, United Kingdom

[*]For correspondence. E-mail leish@mail.hzau.edu.cn

Short running title: Root system architecture of oilseed rape under two phosphate availabilities

Received: 1 February 2016 Accepted: 16 March 2016

<<TYPESETTER: THIS MS HAS EQUATIONS PLEASE INSERT WHERE INDICATED>>

A novel *Brassica*-rhizotron system to unravel the dynamic changes in root system architecture of oilseed rape under phosphorus deficiency

• **Background and Aims** An important adaptation of plants to phosphorus (P) deficiency is to alter root system architecture (RSA) to increase P acquisition from the soil, but soil-based observations of RSA are technically challenging, especially in mature plants. The aim of this study was to investigate the root development and RSA of oilseed rape (*Brassica napus* L.) under low and high soil P conditions during an entire growth cycle.

• **Methods** A new large *Brassic*a-rhizotron system (~118 L volume) was developed to study the RSA dynamics of *B. napus* cv. *Zhongshuang11* in soils, using top-soils supplemented with of low P (LP) or high P (HP) for a full plant growth period. Total root length (TRL), root tip numbers (RTN), root length density (RLD), biomass and seed yield traits were measured.

• **Key Results** TRL and RTN increased more rapidly in HP than LP plants from seedling to flowering stages. Both traits declined from flowering to silique stages, and then increased slightly in HP plants; in contrast, root senescence was observed in LP plants. RSA parameters measured from the polycarbonate plates were empirically consistent with analyses of excavated roots. Seed yield and shoot dry weights were closely associated positively with root dry weights, TRL, RLD and RTN at both HP

and LP.

• **Conclusions** The *Brassica*-rhizotron system is an effective method for soil-based root phenotyping across an entire growth cycle. Given that root senescence is likely to occur earlier under low P conditions, crop P deficiency is likely to affect late water and nitrogen uptake which is critical for efficient resource use and optimal crop yields.

Key words: oilseed rape (*Brassica napus* L.), phosphorus deficiency, root system architecture, dynamic changes, *Brassica*-rhizotron

INTRODUCTION

In plants, phosphorus (P) is a structural element of nucleic acids, enzymes, phosphoproteins and phospholipids, and is involved in energy transfer, enzyme reactions, photosynthesis and carbon partitioning (Marschner, 2012). Plant uptake of P is mainly as inorganic phosphate (Pi), which is typically present at concentrations <10 μM in the soil solution and limited by slow rates of diffusion and mass flow (Bieleski, 1973). In soils, Pi availability to plant roots is limited by strong binding with iron-aluminum oxides in acid environments and by carbonates in calcareous soils (Raghothama, 1999). Strategies for cultivating plants under low soil Pi availability include those aimed at improving P utilisation, and enhancing the acquisition or uptake of P (Vance, 2001), for example, by increasing root growth or altering root system architecture (RSA) for efficient root foraging (White *et al*., 2013).

Under P-limited conditions, *Arabidopsis thaliana* shows inhibition of primary root length (Ticconi *et al*., 2004; Sanchez-Calderon *et al*., 2005; Svistoonoff *et al*., 2007; Fang *et al*., 2009; Giehl *et al*., 2014), stimulation of lateral roots and increased root hair production (Williamson *et al*., 2001; Linkohr *et al*., 2002; Malamy, 2005; Peret *et al*., 2011). The RSA of common bean and soybean is shallow at low P (Bonser *et al*., 1996; Lynch and Brown, 2001, 2008; Rubio *et al*., 2003). In maize (Mollier and Pellerin, 1999; Peng *et al*., 2012) and rice (Fang *et al*., 2009; Zhu *et al*., 2011; Rose *et al*., 2012; Wu *et al*., 2013), more adventitious roots are produced under P deficient conditions. These alternations of RSA traits enhance plant acquisition of P.

Oilseed rape (*Brassica napus* L.) is one of the most important oil crops globally, grown on 36.5 Mha (FAO, http://faostat.fao.org/, 2013). In China, which is the world's leading producer of oilseed rape, 50-70% of oilseed rape cultivated land (~7.52 Mha) in Hubei, Sichuan, Hunan, Anhui, Jiangsu, and Henan Provinces, is severely P-deficient (Yan *et al*., 2006). Under such conditions, oilseed rape growth is inhibited, with purpling of cotyledons and with older leaves becoming dark green at the seedling stage. At maturity, plants have fewer branches and seed setting is low (Ding *et al*., 2012; Shi TX *et al*., 2013a, 2013b). Application of P fertilizers increases the number of plant branches, pod number per plant, seeds per pod, and 1000-seed weight (Cheema *et al*., 2001). In *B. napus* roots, primordia and lateral roots are stimulated and primary root growth is reduced under P-stress at the seedling stage (Akhtar *et al*., 2008; Yang *et al*., 2010; Shi TX *et al*., 2013b). However, root growth

is maintained relative to shoot growth, resulting in increasing root:shoot biomass ratios during early flowering and ripening (Ukrainetz *et al*., 1975; Hermans *et al*., 2006). *Brassica napus* cultivars with high physiological P use efficiency (PPUE) have been shown to have longer lateral root lengths than those cultivars with low PPUE under P-stress (Akhtar *et al*., 2008). In addition, the plant P concentration and the diffusion coefficient of Pi increased at LP by release of large amount of P-mobilizing root exudates, such as citrate, malate or oxalate (Hoffland *et al*., 1989; Zhang *et al.*, 1997; Pearse *et al*., 2006; Wang *et al*., 2013).

The effect of P deficiency on root development and its correlation with plant shoot growth during whole growth of oilseed rape has not yet been reported in detail, potentially for two reasons. First, it is difficult to observe roots in the field nondestructively. Second, the growth period (e.g. ~250 d in Wuhan) makes repeated observations extremely challenging. The aim of this study was to investigate the root development and RSA of oilseed rape (*Brassica napus*) under low and high soil P conditions during an entire growth cycle. This study sought to employ conditions similar to real field environment, and to determine the effects of P applied in the top soil (0-20 cm) on the root growth of oilseed rape at different soil depth. Given the difficulties of studying plant root development and RSA in field soils during an entire growth cycle (Nagel *et al*., 2012, Fender *et al*., 2013), a large rhizotron system was designed and deployed.

MATERIALS AND METHODS

Plant material

The oilseed rape (*Brassica napus* L.) cultivar used in this study was "*Zhongshuang11*", a double low (low gluconsinolate, low erucic acid), semi-winter, commercial cultivar with high potential seed yields, which is grown widely in the middle- and lower-reaches of the Yangzi river in China.

Soil type

The soil used in this study was a grey purple sandy soil, derived from sandy shale, and collected from XinZhou district (Wuhan, China, 28.42° N 112.33° E). The basic agrochemical properties on a dry soil basis were: pH (1:1 H_2O w/v) 7.7, organic carbon (dichromate oxidation method) 1.33 g kg^{-1}, total nitrogen (kjeldahl acid-digestion method) 0.25 g kg^{-1}, available nitrogen (alkali-hydrolyzable nitrogen) 12.7 mg kg^{-1}, total P 0.072 g kg^{-1}, available P (Olsen-P) 4.0 mg kg^{-1} and hot water soluble boron (HWSB) 0.10 mg kg^{-1}. The methods are described by Shi *et al.* (2013b) and Wang *et al.* (2014).

Experimental design

A total of 36 rhizotrons were used in this study. Each rhizotron comprised a container made of polyvinyl chloride (PVC) sheets, whose rear side was a transparent polycarbonate plate. The container was 670 mm width, 180 mm deep and 1000 mm height, giving a volume of ~118 L. A hollow steel tube (⌀50 mm × 7 mm) was used to support the rhizotron, with the tubes fixed to grooves on two parallel walls made of concrete and brick. The rear side of the rhizotron was leant against the steel tube at approximately 15° from the vertical, which allowed the roots

grow along the polycarbonate plate. A black blow molding board was attached to the outside of the polycarbonate plate to create a dark environment for root growth.

Initially, each rhizotron was filled with 120 kg of the same dry soil without fertilization. Soil was sieved to 4 mm. Then, a further 30 kg of the treated soils was added to each rhizotron so that 18 units received 5 mg P_2O_5 kg^{-1} soil (low phosphorus, LP) or 150 mg P_2O_5 kg^{-1} soil (high phosphorus, HP). The depth of topsoil with the contrasting P-treatments was ~200 mm. Ground fertilizers consisted of 200 mg kg^{-1} N ($(NH_4)_2SO_4$), 150 mg kg^{-1} K_2O (KH_2PO_4), and 250 mg kg^{-1} $MgSO_4 \cdot 7H_2O$, respectively were mixed evenly with topsoil. Next, 30 mL of micronutrient solution with 2.84 g L^{-1} H_3BO_3, 1.80 g L^{-1} $MnCl_2$ $4H_2O$, 0.22 g L^{-1} $ZnSO_4 \cdot 7H_2O$, 0.08 g L^{-1} $CuSO_4 \cdot 5H_2O$ and 0.024 g L^{-1} $Na_2MoO_4 \cdot 2H_2O$, and 30 mL 0.05 mmol L^{-1} Fe-EDTA was applied uniformly to the topsoil. Finally, each rhizotron was irrigated pre-sowing with 6 L distilled H_2O. The bulk density of soil was 1.4 g cm^{-3} and the gravimetric moisture content was 120 g kg^{-1}. A groove in the topsoil 60 cm long, 1 cm wide, 2 cm deep and 2 cm from the glass plate was made in each rhizotron, and 30 seeds were sown evenly in the groove and covered lightly with soil. Each rhizotron was covered with a thin plastic film until the seeds germinated (~2 d). The seeds were sown on Oct. 23th 2013. Two weeks after germination, seedlings were thinned to nine plants per rhizotron, and after a further three weeks, thinned to three plants per rhizotron.

The rhizotrons were arranged in a fully randomized design with three replications. A total of 27 plants at the seedling stage and nine plants during the budding, bolting,

flowering, silique and ripening stages of each treatment were sampled respectively. Because P deficiency delayed the reproductive growth period of oilseed rape, sampling times at LP were delayed by 22 d at budding stage, 6 d at bolting stage and 1 d at flowering stage.

Root system architecture (RSA) analysis and data collection

(1) Polycarbonate plate root system architecture

Before sampling, the black blow molding boards attached to the polycarbonate plate were removed and polyester paper (670 mm wide × 1000 mm long) was attached to the glass plate. The root morphology was then traced with a marker with 0.2 mm width (Creative Wealth Stationery Co., ltd, Shaoguan, Guangdong, China). The whole root and two edges of the wider roots were all traced. Each sheet of polyester paper was then scanned with A0 size scanner (SmartLF GX+42C, Colortrac, Cambridge, UK) and a gray scale image was taken at a resolution of 400 dpi. Images were saved in JPG format and then converted to BMP format by image binarization with ArcMap V9 software (ArcGIS, Environmental Systems Research Institute, Inc., Redlands, CA, USA). Total root length (TRL, m) and the number of root tips (RTN) were determined with WinRHIZO program (Regent Instruments Inc., Quebec, Canada). Root length from the top to the bottom of each image was calculated in 5 cm sections and *polycarbonate plate* root length density (RLD, mm/mm^2) = root length (mm) / analyzed area (mm^2).

(2) Excavated root system architecture

After shoots were sampled, the polycarbonate plate was removed. The entire root system was taken out of the soil carefully and cleaned with tap water once and distilled H_2O twice immediately. Root diameter distributions were measured using Vernier calipers (Everpower-557115, Lishui, Guangdong, China). First, lateral roots were cut from the main root. For each lateral root, the diameter was measured at the point of intersection with the main root in three rotational positions. Then, the root was put in a clear perspex tray with a film of distilled H_2O and scanned with a modified flatbed scanner (Epson V700, Nagano-ken, Japan) at 400 dpi. Larger root systems were divided into several sections and scanned one-by-one. The images of roots were analyzed with WinRHIZO software (Regent Instruments Inc., Quebec, Canada).

Agronomic traits

(1) Biomass measurement

From seedling to flowering stages, the plants were divided into shoot, (mature) hypocotyl and root, respectively, and the samples were cleaned with distilled H_2O. Because almost all the leaves had senesced at silique stage, typical of oilseed rape, the shoot was divided into pod and straw at silique stage; and straw, pericarp and seed at harvest stage, respectively. Samples were oven-dried at 105°C for 30 min, then at 65°C for 48 h, to constant mass. Dried samples were weighed and ground to a powder for P determination in a micro plant grinding machine (Taisite-FZ102,

Jinghai, Tianjin, China).

(2) Seed-yield and yield-related traits

Plant height (PH) and branch number (BN) per plant were measured before harvest. Stems were then cut, pod number (PN) per plant and pod number of main inflorescence (PNM) were counted. 25 siliques from each plant were sampled randomly and seed numbers counted. After a subsequent ripening period (typically two weeks), all siliques from each plant were threshed and total seed yield and 1000-seed weight determined.

(3) Determination of tissue P concentration

A micro-Kjeldahl method was used to determine P concentration in plant tissues. First, 0.1 g ground sample and 5 mL 98% H_2SO_4 were added into a 50 mL digestion tube and shaken for 10 h. Then, the digestion tube was put in the heating block and digested at 250°C for 2 h with 5-10 drops of H_2O_2 added. Finally, 4 mL digested solution from each tube was taken out and diluted with 6 mL distilled water to determine P concentration using a Continuous-Flow injection analyzer (AA3, Seal Analytical GmbH, Bran, Germany).

Calculations and analysis

The following equation was used to calculate the physiological P use efficiency according to Hammond *et al* (2009).

<<TYPESETTER:PLEASE INSERT EQUATION 1 HERE>>

Statistical analyses

We used Genstat®V16 (VSN International, Oxford, UK) to analyze the data. Analysis of variance (ANOVA) was used to identify significant differences (P= 0.05) in the investigated traits among treatments and growth periods. The least significant difference (LSD) had also been conducted to test the significant difference in the root length density in the same soil depth between LP and HP. Figures were made using Sigma Plot 11 (Systat Software Inc., Chicago, Illinois).

RESULTS

Large rhizotron system enables efficient phenotyping root system architecture

Polycarbonate plate root system architecture (plate RSA) including total root length (TRL) and the number of root tips (RTN) (Fig. 2B, D) showed similar trends to excavated-RSA traits (Fig. 2A, C) during the entire growth cycle. Both plate RSA and excavated RSA traits indicated that P deficiency inhibited root development during the entire growth cycle except for TRL and RTN based on plate RSA at silique stage (Fig. 2).

At LP, the maximum values of TRL and RTN of excavated-RSA and plate RSA traits occurred at the silique stage (Fig. 2). However, at HP, the maximum values of excavated-RSA traits were observed at flowering stage and plate RSA traits at the bolting stage (Fig. 2). Although, there was no significant difference observed in RTN of plate RSA traits at LP from budding to flowering stages, an increase in both of

excavated-RSA traits was observed during this period.

Root system architecture (RSA) of cv. Zhongshuang 11 during growth under contrasting phosphate availabilities

The TRL and RTN increased rapidly at HP from the seedling stage and reached a maximum at flowering stage (Fig. 2A, C). These root traits then declined from flowering to silique stages and finally increased slightly from silique to harvest stages. In contrast, TRL and RTN at LP increased much more slowly from seedling to silique stages, and then decreased significantly from silique to harvest stages (Fig. 2A, C). Both TRL and RTN at HP were higher than at LP throughout growth, notably at flowering and ripening stages.

Total root number and root number within each diameter range of 2-5 mm and 5-10 mm decreased from flowering to silique stages, and then increased from silique to harvest stages at HP (Fig. 3A), however, no significant differences were observed in all above-mentioned root traits at LP. Moreover, root numbers within each diameter range, e.g. 2-5 mm, 5-10 mm, >10 mm at LP were lower than that at HP for each growth period (Fig. 3A). Roots in the diameter range 2-5 mm accounted for around 50% of the total root number at both LP and HP. In addition, RDW of each root diameter range of <2 mm, 2-5 mm, 5-10 mm and >10 mm were greater at HP than at LP in flowering, silique and ripening stages (Fig. 3B). RDW within root diameter range >10 mm accounted for approximately 60% of the total DW at HP and 50% of the total DW at LP.

Dynamic changes in root length density (RLD) in different soil depths occurred throughout growth in both P treatments (Fig. 4). At the seedling stage, peak RLD occurred in soil depth of 10 cm in both P treatments. RLD then declined sharply from soil depth of 10 cm to 40 cm in both P treatments. The RLD at HP was much greater than at LP from soil depths 0 to 25 cm, but slightly less than at LP from soil depths 30 to 45 cm (Fig. 4A). From budding to harvest stages, there were two peaks of RLD, one in soil depth of ~20 cm and another ranged in soil depths 60 to 80 cm, under both P conditions (Fig. 4B-F). The RLD at HP was greater than that at LP in almost all the soil layers from budding to flowering stages. At the silique stage, RLD at LP was slightly greater than at HP from soil depth 0 to 30 cm. However, there were no significant differences in RLD between LP and HP treatments from soil depths 30 to 75 cm at the silique stage (Fig. 4E). At the ripening stage, there was no significant difference in RLD between LP and HP from soil depths 0 to 15 cm, RLD at HP was slightly higher than that at LP from soil depths 20 cm to 80 cm (Fig. 4F).

The average RLD of ZS11 at HP increased markedly from 0.015 mm mm^{-2} at seedling stage to 0.098 mm mm^{-2} at the bolting stage. It then declined to 0.058 mm mm^{-2} at the silique stage and finally increased to 0.070 at the ripening stage. The average RLD at LP increased constantly from 0.012 mm mm^{-2} at the seedling stage to 0.064 mm mm^{-2} at the silique stage, and then it decreased to be 0.053 mm mm^{-2} at ripening stage (Table 1). On the basis of this contrasting P availability in the top soil together with dynamic variation of RLD in different soil depths, the spatial distribution of RSA varied significantly with root development in soil at both LP and

HP. These results show that our rhizotron system can be used to identify valuable root traits related to P accessibility.

Root and shoot biomass of cv. Zhongshuang 11 during growth under contrasting phosphate availabilities

Root dry weight (RDW) at HP was significantly greater than at LP throughout the entire growth period (Fig. 5A). RDW at HP increased rapidly from seedling to bolting stages and then increased slowly from bolting to silique stages, and finally declined slightly from silique to ripening stages. However, at LP, RDW increased slowly from seedling to flowering stages, then decreased rapidly from flowering to silique stages, and finally increased from silique to ripening stages (Fig. 5A).

Shoot dry weight (SDW) at HP increased rapidly from seedling to bolting stages and then increased more slowly from bolting to silique stages, and finally decreased slightly from silique to ripening stages (Fig. 5B). At LP, SDW increased slowly from seedling to silique stages, then decreased slightly from silique to ripening stages, which in contrast to the increased trend of RDW at silique stage (from flowering to ripening stages) at LP (Fig. 5B). At HP, the DW of pod and straw at silique stage and DW of pericarp, seed, and straw at ripening stage were greater than that at LP (Fig. 5C).

The root:shoot biomass ratio (R/S ratio) increased considerably from seedling to flowering stages at HP, while at LP, the R/S ratio firstly declined slightly from seedling to budding stages, then increased from budding to flowering stages. At both

LP and HP, R/S ratio declined from flowering to silique stages and finally increased slightly from silique to ripening stages (Fig. 5D). The R/S ratios at LP were significantly greater than those at HP from seedling to bolting stages, and were much less than at HP from silique to ripening stages (Fig. 5D).

Seed yield of ZS11 at HP was about three times greater than at LP (Table 2). Almost all the yield components at LP were far less than that at HP, such as number of primary branches per plant (BN), pod number per plant (PN), 1000-seed weight, seed number per pod (SN), yet, the height to the first primary branch (FBH) at LP (56.3±1.6 cm) was slight higher than that at HP (48.4±2.5 cm). There was no significant difference in pod number of main inflorescence (PNM) between LP and HP.

Physiological phosphorus use efficiency of cv. Zhongshuang 11 during growth under contrasting phosphate availabilities

Root and (mature) hypocotyl P concentration decreased continually from seedling to ripening stages at both LP and HP (except at budding stage at HP). Additionally, root and (mature) hypocotyl P concentrations at LP were less than those at HP, notably from seedling to late flowering stages (Fig. 6A, B). Root P content increased considerably from seedling to bolting stages, and then declined to silique stage at HP (Table 3). Root P content increased from seedling to budding stages at LP, then progressed slightly from budding to silique stages, and finally declined a little from silique to harvest stages. During the entire growth period, both root and (mature)

hypocotyl P content at LP were much lower than those at HP (Table 3).

Shoot P concentration at HP decreased from seedling to bolting stages, and then increased slightly from bolting to flowering stages (Fig. 6C). In contrast, shoot P concentration at LP decreased sharply from seedling to budding stages, and then continued to decline from budding to flowering stages. Shoot P concentration at HP was greater than at LP from seedling to flowering stages, and shoot P contents at HP were far higher than at LP during the whole growth period except for at early seedling stage. Pod and seed accounted for high proportion in P concentrations and contents at silique and ripening stages (Fig. 6D).

Physiological P use efficiency (PPUE) of roots increased more rapidly at HP than at LP from budding to ripening stages (Fig. 7A). The PPUE of (mature) hypocotyl were much greater at HP than at LP from flowering to ripening stages (Fig. 7B). Shoot PPUE increased from seedling to bolting stages at HP, and then declined slightly from bolting to flowering stages (Fig. 7C). At LP, PPUE of shoot increased much slowly than at HP from seedling to flowering stages. The PPUE of pod and straw at silique stage, straw and seed at ripening stage, were much higher at HP than at LP (Fig. 7D).

DISCUSSION

Brassica-rhizotron system

Several approaches for phenotyping root system architecture (RSA) from lab to field have been developed. Plants grown in a nutrient solution (Gericke, 1937; Yang *et al*.,

2010), paper culture (Hammond *et al*., 2009; Yang *et al*., 2010; Adu et al. 2014; Thomas et al., 2016) or clear gel media (Bengough *et al*., 2004; Iyer-Pascuzzi *et al*., 2010; Shi *et al*., 2013c) can be used to remove the influence of complex soil environments on root growth. Plants cultivated in sand-filled pots or PVC tubes could be used to predict root development of plants in more complex substrates (Zhu *et al*., 2011). In the field, transparent tubes (minirhizotrons) can be used to investigate the roots which touch the tube and so can be well-suited for studying fine roots (Iyer-Pascuzzi *et al*., 2001). Additionally, wall techniques or root windows can be used to create an observing plane to detect root growth along soil profiles (Polomski and Kuhn, 2002). Other promising technologies, such as X-ray computed tomography (CT) or Magnetic resonance imaging (MRI) are promising tools for visualizing plant root systems within their natural soil environment noninvasively (Tracy *et al*., 2010; Mairhofer *et al*., 2012). The overarching characteristic of RSA studies in the field is that it is logistical challenging to adequately assess RSA throughout growth. Utilizing and combining different imaging systems, integrating measurements and image analysis where possible, and amalgamating data will allow researchers to gain a better understanding of root:soil interactions (Downie, *et al*., 2015).

The *Brassica*-rhizotron system used in this study was specifically designed to satisfy routine evaluation of roots growth of oilseed rape in soil environment throughout an entire growth period (Fig. 1). Whilst most of the roots of oilseed rape would be expected reach the transparent plate due to gravitropism, two or three

lateral roots of each plant did not touch the transparent plate. Furthermore, during plant development, the ratio of the roots observed at the transparent plate decreased. However, at both P levels, dynamic changes of TRL and RTN observed on the polycarbonate plate-RSA exhibited the same trend with the parameters of excavated-RSA during the whole growth stage (Fig. 2). These indicated that our rhizotron system could be used to conduct non-destructive root system phenotyping using polycarbonate plate RSA root parameters as a proxy.

Root system growth

Allen and Morgan (1975) identified two phases of root growth in oilseed rape, one up to anthesis and another 2 weeks post-anthesis. Other studies demonstrated that root biomass of oilseed rape progressed to the maximum at late-flowering (Gan *et al*., 2009) or silique stages (Wang *et al*., 2014) and then decreased. Our study indicated that the maximum value of RDW occurred at the silique stage at HP, but occurred earlier at LP, at the flowering stage (Fig. 5A). However, the DW of lateral roots with diameter <2 mm, 2-5 mm, 5-10 mm and 10-15 mm was much higher at flowering than at silique stage at both P levels (Fig. 3B). These indicated that lateral root, rather than primary root, plays a vital role in the construction of root morphology and root biomass. Root length density of oilseed rape typically decreases exponentially with soil depth (Yu *et al*., 2007; Whalley *et al*., 2008; Liu *et al*., 2011). In our study, the decrease in RLD was not smooth from bolting to silique stages (Fig. 4), which was probably attributed to the water and nutrients movement and

distribution in the soil affected by irrigation (White and Kirkegaard 2010; Jin *et al*., 2015).

Effect of low phosphorus on the root and shoot growth of oilseed rape

Root and shoot biomass was less under P deficiency throughout the entire growth period. Moreover, the difference between the two P treatments increased during growth (Fig. 5). Lower biomass accumulation could be the result of reduced net photosynthesis (source limitation), but may also be due to direct negative effects of low P availability on growth (sink limitation). Reductions in root growth of rice under P deficiency were not caused by source limitations, but were due to a more direct effect of low P availability on growth. Even at sub-optimal tissue P concentrations <0.7 mg P g^{-1} DW, plants are able to produce enough assimilates to sustain growth that is limited directly by low P availability (Wissuwa *et al*. 2005). In this study, the P concentrations of (mature) hypocotyl, root and shoot were far more than 0.7 mg P g^{-1} DW from seedling to flowering stages (Fig. 6A-C). During the silique and ripening stages, although the straw concentration were less than 0.7 mg P g^{-1} DW, there were no significant differences in the straw concentration between at LP and at HP (Fig. 6D).

The R/S ratio reached a maximum value at the flowering stage at both LP and HP. Moreover, the R/S ratios at LP were much higher than that at HP from seedling to bolting stages (Fig. 5D). The increase in R/S ratio under P starvation is due to the increase in partitioning of carbohydrates towards the roots (Fredeen *et al*., 1989;

Hermans *et al*., 2006; Hammond and White, 2008, 2011). Observations showed that both root and shoot growth are directly affected by Pi availability and that the increase in R/S ratio frequently observed under P deficiency is causally due to P rather than carbohydrate partitioning to roots (Wissuwa et al., 2005). However, in this study, the R/S ratios at LP were much lower than at HP from flowering to ripening stages (Fig. 5D). The reason could be attributed to reduction of RDW and relatively higher increase of SDW at LP as compared with that at HP (Fig. 5 A and B). This pattern suggested that root growth is tightly associated with shoot development during the early vegetative period and then the relationship weakens during the reproductive growth stage, which is consistent with previous studies (Snapp and Shennan, 1992; Wells and Eissenstat, 2003; Peng *et al*., 2010). Total root length (TRL), root tip number (RTN) and root length density (RLD) of oilseed rape were reduced under P deficiency across almost all growth stages (Figs. 2 and 5; Table 1), and decreased P uptake (Fig. 6) and root growth (Fig. 5), leading to reduced shoot growth (Fig. 5), PPUE of tissues (Fig. 7) and seed yield (Table 2). Large amounts of photosynthate are likely to be transferred preferentially to developing pods on the main inflorescence, rather than to maintain root growth under low P stress at pod-filling stage (Fig. 5; Table 2).

Conclusions

Our new large rhizotron system (~118 L) provides an effective and efficient method to study dynamic RSA of oilseed rape across an entire growth period, which

therefore helps to bridge the gap between lab and field study of roots. Total root length, root tip number, root and shoot DW of oilseed rape under P deficient condition were reduced throughout growth. Interestingly, P deficiency also showed that root senescence is likely to occur earlier under low P conditions, which is crucial for water and mineral nutrients uptake and the production of seed yield (Blum, 2005; Foulkes *et al*., 2009; White *et al*., 2015).

ACKNOWLEDGMENTS

The authors acknowledge the financial support from National Nature Science Foundation of China (grant number 31471933), New Century Excellent Talents in University of Ministry of Education of China (grant number NCET-13-0809), Natural and Fundamental Research Funds for the Central Universities of China (grant numbers 2012PY006 and 2014PY020).

LITERATURE CITED

Adu MO, Chatot A, Wiesel L, Bennett MJ, Broadley MR, White PJ, Dupuy LX. 2014. A scanner system for high-resolution quantification of variation in root growth dynamics of *Brassica rapa* genotypes. *Journal of Experimental Botany* **65**: 2039-2048.

Akhtar MS, Oki Y, Adachi T. 2008. Genetic variability in phosphorus acquisition and utilization efficiency from sparingly soluble P-sources by Brassica cultivars under P-stress environment. *Journal of Agronomy and Crop Science* **194**: 380-392.

Allen EJ, Morgan DG. 1975. A quantitative comparison of the growth, development and yield of different varieties of oilseed rape. *The Journal of Agricultural Science* **85**: 159-174.

Bengough AG, Gordon DC, Al-Menaie H, Ellis RP, Allan D, Keith R, Thomas WTB, Forster BP. 2004. Gel observation chamber for rapid screening of root traits in cereal seedlings. *Plant and Soil* **262**: 63-70.

Bieleski RL. 1973. Phosphate pools, phosphate transport, and phosphate availability. *Annual*

Review of Plant Physiology **24**: 225-252.

Blum A. 2005. Drought resistance, water-use efficiency, and yield potential—are they compatible, dissonant, or mutually exclusive? *Australian Journal of Agricultural Research* **56**: 1159-1168.

Bonser AM, Lynch J, Snapp S. 1996. Effect of phosphorus deficiency on growth angle of basal roots of *Phaseolus vulgaris*. *New Phytologist* **132**: 281-288.

Cheema MA, Malik MA, Hussain A, Shah SH, Basra SMA. 2001. Effects of time and rate of nitrogen and phosphorus application on the growth and the seed and oil yields of canola (*Braaica napus* L.). *Journal of Agronomy and Crop Science* **186**: 103-110.

Ding GD, Zhao ZK, Liao Y, Hu YF, Shi L, Long Y, Xu FS. 2012. Quantitative trait loci for seed yield and yield-related traits, and their responses to reduced phosphorus supply in *Brassica napus*. *Annals of Botany* **109**: 747-759.

Downie HF, Adu MO, Schmidt S, *et al*. 2015. Challenges and opportunities for quantifying roots and rhizosphere interactions through imaging and image analysis. *Plant, Cell & Environment* **38:** 1213-1232.

Fang Z, Shao C, Meng Y, Wu P, Chen M. 2009. Phosphate signaling in *Arabidopsis* and *Oryza sativa*. *Plant Science* **176**: 170-180.

Fender AC, Gasert D, Jungkunst HF, *et al*. 2013. Root-induced tree species effects on the source/sink strength for greenhouse gasses (CH_4, N_2O and CO_2) of a temperate deciduos forest soil. *Soil Biology and Biochemistry* **57**: 587-597.

Foulkes MJ, Hawkesford MJ, Barraclough PB, Holdsworth MJ, Kerr S, Kightley S, Shewry PR. 2009. Identifying traits to improve the nitrogen economy of wheat: recent advances and future prospects. *Field Crops Research* **114**: 329-342.

Fredeen AL, Rao IM, Terry N. 1989. Influence of phosphorus nutrition on growth and carbon partitioning in Glycine max. *Plant Physiology* **89**: 225-230.

Gan YT, Campbell CA, Janzen HH, Lemke R, Liu LP, Basnyat P, McDonald CL. 2009. Root mass for oilseed and pulse crops: growth and distribution in the soil profile. *Canadian Journal of Soil Science* **80**: 179-192.

Gericke WF. 1937. Hydroponics-crop production in liquid culture media. *Science* **85**: 177-178.

Giehl RFH, Gruber BD, von Wiren N. 2014. It's time to make changes: modulation of root system architecture by nutrient signals. *Journal of Experimental Botany* **65**: 769-778.

Hammond JP, Broadley MR, White PJ, *et al*. 2009. Shoot yield drives phosphorus use efficiency in *Brassica oleracea* and correlates with root architecture traits. *Journal of Experimental Botany* **60**: 1953-1968.

Hammond JP, White PJ. 2008. Sucrose transport in the phloem: integrating root responses to phosphorus starvation. *Journal of Experimental Botany* **59**: 93-109.

Hammond JP, White PJ. 2011. Sucrose signaling in root responses to low phosphorus

availability. *Plant Physiology* **156**: 1033-1040.

Hermans C, Hammond JP, White PJ, Verbruggen N. 2006. How do plants respond to nutrient shortage by biomass allocation? *Trends in Plant Science* **11**: 610-617.

Hoffland E, Findenegg GR, Nelemans JA. 1989. Solubilization of rock phosphate by rape. Ⅱ. Local root exudation of organic acids as a response to P starvation. *Plant and Soil* **113**: 161-165.

Iyer-Pascuzzi AS, Symonova O, Mileyko Y, *et al.* 2001. Advancing fine root research with minirhizotrons. *Environmental and Experimental Botany* **45**: 263-289.

Iyer-Pascuzzi AS, Symonova O, Mileyko Y, *et al.* 2010. Imaging and analysis platform for automatic phenotyping and trait ranking of plant root systems. *Plant Physiology* **152**: 1148-1157.

Jin KM, Shen JB, Ashton RW, *et al.* 2015. Wheat root growth responses to horizontal stratification of fertiliser in a water-limited environment. *Plant and Soil* **386**: 77-88.

Liu LP, Gan YT, Bueckert R, Rees KV. 2011. Rooting systems of oilseed and pulse crops. II: vertical distribution patterns across the soil profile. *Field Crops Research* **122**: 248-255.

Lynch JP, Brown KM. 2001. Topsoil foraging- an architectural adaptation of plants to low phosphorus availability. *Plant and Soil* **237**: 225-237.

Lynch JP, Brown KM. 2008. Root strategies for phosphorus acquisition. In: White PJ, Hammond JP, eds. *The ecophysiology of plant-phosphorus interactions*. Dordrecht, the Netherlands: Springer, 83-116.

Mairhofer S, Zappala S, Tracy SR, *et al.* 2012. RooTrak: Automated recovery of three-dimensional plant root architecture in soil from X-ray microcomputed tomography images using visual tracking. *Plant Physiology* **158**: 561–569.

Malamy JE. 2005. Intrinsic and environmental response pathways that regulate root system architecture. *Plant, Cell and Environment* **28**: 67-77.

Marschner H. 2012. Mineral nutrition of higher plants. 3nd edn. London: Academic Press.

Mollier A, Pellerin S. 1999. Maize root system growth and development as influenced by phosphorus deficiency. *Journal of Experimental Botany* **50**: 487-497.

Nagel KA, Putz A, Gilmer F, *et al.* 2012. Growscreen-rhizo is a novel phenotyping robot enabling simultaneous measurements of root and shoot growth for plants grown in soil-filled rhizotrons. *Functional Plant Biology* **39**: 891-904.

Pearse SJ, Veneklass EJ, Cawthray GR, Bolland MDA, Lambers H. 2006. Carboxylate release of wheat, canola and 11 grain legume species as affected by phosphorus status. *Plant and Soil* **288**: 127-139.

Peng YF, Niu JF, Peng ZP, Zhang FS. 2010. Shoot growth potential drives N uptake in maize plants and correlates with root growth in the soil. *Field Crops Research* **115**: 85-93.

Peng YF, Yu P, Zhang Y, *et al.* 2012. Temporal and spatial dynamics in root length density of field-grown maize and NPK in the soil profile. *Field Crops Research* **131**: 9-16.

Peret B, Clement M, Nussaume L, Desnos T. 2011. Root developmental adaptation to phosphate starvation: better safe than sorry. *Trends in Plant Science* **16**: 442-450.

Polomski J, Kuhn N. 2002. Root research methods. In: Wsisel Y *et al*., eds. *Plant roots the hhiden half*, 3rd edn. New York, USA: Marcel Dekker, 295-321.

Raghothama KG. 1999. Phosphate acquisition. *Annual Review of Plant Physiology and Plant Molecular Biology* **50**: 665-693.

Rose TJ, Impa SM, Rose MT, *et al.* 2012. Enhancing phosphorus and zinc acquisition efficiency in rice: a critical review of root traits and their potential utility in rice breeding. *Annals of Botany* **112**: 331-345.

Rubio G, Liao H, Yan X, Lynch JP. 2003. Topsoil foraging and its role in plant competitiveness for phosphorus in common bean. *Crop Science* **43**: 598-607.

Sanchez-Calderon L, Lopez-Bucio J, Chacon-Lopez A, *et al.* 2005. Phosphate starvation induces a determinate developmental program in the roots of *Arabidopsis thaliana*. *Plant and Cell Physiology 46*: 174-174.

Shi TX, Li RY, Zhao ZK, *et al.* 2013a. QTL for yield traits and their association with functional genes in response to phosphorus deficiency in *Brassica napus*. *PLoS One* **8**: e54559.

Shi TX, Zhao DY, Li DX, *et al.* 2013b. *Brassica napus* root mutants insensitive to exogenous cytokinin show phosphorus efficiency. *Plant and Soil* **358**: 61-74.

Shi L, Shi TX, Broadley MR, *et al.* 2013c. High throughput root phenotyping screens identify genetic loci associated with root architectural traits in *Brassica napus* under contrasting phosphate availabilities. *Annals of Botany* **112**: 381-389.

Snapp S, Shennan C. 1992. Effects of salinity on root growth and death dynamics of tomato *Lycopersicon esculentum* Mill. *New Phytologist* **121**: 71-79.

Svistoonoff S, Creff A, Reymond M, *et al.* 2007. Root tip contact with low-phosphate media reprograms plant root architecture. *Nature Genetics* **39**: 792-796.

Ticconi CA, Delatorre CA, Lahner B, Salt DE, Abel S. 2004. *Arabidopsis* pdr2 reveals a phosphate-sensitive checkpoint in root development. *The Plant Journal* **37**: 801-814.

Thomas CL, Graham NS, Hayden R, Meacham MC, Neugebauer K, Nightingale M, Dupuy LX, Hammond JP, White PJ, Broadley MR. 2016. High throughput phenotyping (HTP) identifies seedling root traits linked to variation in seed yield and nutrient capture in field-grown oilseed rape *(Brassica napus* L.). *Annals of Botany*, in press.

Tracy SR, Roberts JA, Black CR, Mcneill A, Davidson R, Mooney SJ. 2010. The X-factor: visualizing undisturbed root architecture in soils using X-ray computed tomography. *Journal of Experimental Botany* **61**: 311-313.

Ukrainetz H, Soper RJ, Nyborg M. 1975. Plant nutrient requirements of oilseed and pulse

crops. In: Harapiak JT. ed. *Oilseed and pulse crops in western Canada- a symposium.* Calgary, Alberta: Western Cooperative Fertilizers Ltd, 325-374.

Vance CP. 2001. Symbiotic nitrogen fixation and phosphorus acquisition: plant nutrition in a world of declining renewable resources. *Plant Physiology* **127**: 390-397.

Wang Y, Liu T, Li XK, Ren T, Cong RH, Lu JW. 2014. Nutrient deficiency limits population development, yield formation, and nutrient uptake of direct sown winter oilseed rape. *Journal of Integrative Agriculture***14**: 670-680.

Wells CE, Eissenstat DM. 2003. Beyond the roots of young seedlings: the influence of age and order on fine root physiology. *Plant Growth Regulation* **21**: 324-334.

White CA, Sylvester-Bradley R, Berry PM. 2015. Root length densities of UK wheat and oilseed rape crops with implications for water capture and yield. *Journal of Experimental Botany* **66**: 2293-2303.

Whalley WR, Watts CW, Gregory AS, *et al.* 2008. The effect of soil strength on the yield of wheat. *Plant and Soil* **306**: 237-247.

White PJ, George TS, Gregory PJ, Bengough GA, Hallett PD, McKenzie BM. 2013. Matching roots to their environment. *Annals of Botany* **112**: 207-222.

White RG, Kirkegaard JA. 2010. The distribution and abundance of wheat roots in a dense, structured subsoil-implications for water uptake. *Plant, Cell and Environment* **33**: 133-148.

Williamson LC, Ribrioux SPCP, Fitter AH, Leyser HMO. 2001. Phosphate availability regulates root system architecture in *Arabidopsis*. *Plant Physiology* **126**: 875-882.

Wissuwa M, Gamat G, Ismail AM. 2005. Is root growth under phosphorus deficiency affected by source or sink limitations? *Journal of Experimental Botany* **56**: 1943-1950.

Wu P, Shou HX, Xu GH, Lian XM. 2013. Improvement of phosphorus efficiency in rice on the basis of understanding phosphate signaling and homeostasis. *Current Opinion in Plant biology* **16**: 205-212.

Yang M, Ding GD, Shi L, Feng J, Xu FS, Meng JL. 2010. Quantitative trait loci for root morphology in response to low phosphorus stress in *Brassica napus*. *Theoretical and Applied Genetics* **121**: 181-193.

Yan XL, Wu P, Ling HQ, Xu GH, Xu FS, Zhang QF. 2006. Plant nutriomics in China: An overview. *Annals of Botany* **98**: 473-482.

Yu GR, Zhuang J, Nakayama K. 2007. Root water uptake and soil water profile as affected by vertical root distribution. *Plant Ecology* **189**: 15-30.

Zhang FS, Ma J, Cao YP. 1997. Phosphorus deficiency enhances root exudation of low-molecular weight organic acids and utilization of sparingly soluble inorganic phosphates by radish (*Raphanus sativus* L.) and rape (*Brassica napus* L.) plants. *Plant and Soil* **196**: 261-264.

Zhu J, Ingram PA, Benfey PN, Elich T. 2011. From lab to field, new approaches to

phenotyping root system architecture. *Current Opinion in Plant Biology* **14**: 310-317

TABLE 1. *Root length density of cv. Zhongshuang 11 (Brassica napus L.) at LP (low phosphorus) and at HP (high phosphorus)*

	Growth Stage					
	Seedling	Budding	Bolting	Flowering	Silique	Ripening
HP	0.015±0.002 a	0.062±0.005 a	0.098±0.009 a	0.079±0.002 a	0.058±0.0006 a	0.070±0.0009 a
LP	0.012±0.0006 a	0.029±0.003 b	0.037±0.003 b	0.041±0.005 b	0.064±0.001 b	0.053±0.006 b

Note: Root length density ($mm \cdot mm^{-2}$) = total root length (mm) / total root area (mm^2) . Values are mean±SE of 27 plants at the seedling stage and nine plants during the budding, bolting, flowering, silique and ripening stages. Different lower case letters denote significant difference ($P< 0.05$) among treatments.

TABLE 2. *Seed yield and yield components of cv. Zhongshuang 11 (Brassica napus L.) at LP (low phosphorus) and at HP (high phosphorus)*

	LP	HP
SY	11.6±0.8 b	35.6±1.7 a
BN	4.0±0.3 b	8.7±0.6 a
PN	141.3±17.4 a	368.0±31.4 a
PNM	62.0±3.9 a	66.2±4.6 a
SW	3.4±0.1 b	4.0±0.1 a
SN	21.1±0.9 b	23.6±0.3 a

Note: Seed yield (g; SY), number of primary branches per plant (n; BN), pod number per plant (n; PN), pod number of main inflorescence (n; PNM), seed weight of 1,000 seeds (g per 1000 seeds; SW), seed number per pod (n; SN). Values are mean ± SE of nine plants. Different lower case letters denote significant difference ($P < 0.05$) among treatments.

TABLE 3. P content *of cv. Zhongshuang 11 (Brassica napus L.) at LP (low phosphorus) and at HP (high phosphorus).*

Growth stages	Shoot		Root		Crown	
	HP	LP	HP	LP	HP	LP
Seedling	3.26±0.09a	0.53±0.01b	0.19±0.04a	0.08±0.01b	0.17±0.01a	0.03±0.01b
Budding	105.26±16.97a	12.51±2.89b	16.68±1.08a	3.01±0.33b	4.61±1.34a	0.03±0.08b
Bolting	226.30±21.47a	29.14±2.86b	34.45±9.35a	3.53±0.01b	9.20±0.91a	1.30±0.28b
Flowering	246.29±19.52a	45.10±5.08b	18.80±2.79a	3.55±1.13b	9.50±0.48a	1.93±0.72b
Silique	214.70±16.44a	64.94±2.21b	7.39±0.46a	3.65±0.98b	1.86±0.42a	0.45±0.06b
Ripening	291.44±12.45a	165.81±33.57b	9.02±0.01a	1.95±0.82b	0.78±0.01a	0.29±0.05b

Note: Values are mean±SE of 27 plants at the seedling stage and nine plants during the budding, bolting, flowering, silique and ripening stages. Different lower case letters denote significant difference ($P< 0.05$) among treatments.

FIG. 1. Rhizotron. (A) The container (up to a volume of ~118 L) (1) with dimensions 670 mm wide×180 mm deep×1000 mm height has a piece of transparent polycarbonate attached (1b), a hollow steel tube ¢ 50 mm×7 mm used to support the rhizotron (2) and two concrete-sustained walls (850 mm height) with grooves (3) 1a, a drain valve; 1d, screw; 1e, clamp. (B) An installation diagram of the rhizotron. 1b, transparent polycarbonate; 1c, a piece of black blow molding board; 1e, clamp. (C) Polycarbonate plate root system architecture (plate RSA) of Zhongshuang 11 (*Brassica napus* L.) at the budding stage at high phosphorus (HP), 134 d after sowing. Primary roots (ⅰ) and lateral (ⅱ) roots are indicated. (D) The BMP format image of plate RSA.

FIG. 2. Dynamics of total root length (A, B) and root tip number (C, D) of *cv. Zhongshuang 11* (*Brassica napus* L.) grown in rhizotrons at low (LP) and high (HP) phosphorus treatments. A and C show the root traits excavated from soil. B and D show the root traits traced on the polycarbonate plate. Values are mean±SE of 27 plants at the seedling stage and nine plants during the budding, bolting, flowering, silique and ripening stages. The error bars indicate the standard error of the mean.

FIG. 3. Number (A) and dry weight (B) of lateral roots of different diameter ranges of *cv. Zhongshuang 11* (*Brassica napus* L.) at low (LP) and high (HP) phosphorus treatments, from flowering to ripening stages from excavated soils. Fig. 3 A does not include numbers of lateral roots with diameter <2 mm because they are too numerous to calculate. Values are mean±SE of 27 plants at the seedling stage and nine plants during the budding, bolting, flowering, silique and ripening stages. Different lower case letters on right side of the bar denote significant difference ($P< 0.05$; Fisher LSD) within a given diameter class.

FIG. 4. Root length density of *cv. Zhongshuang 11* (*Brassica napus* L.) at different soil depths at low (LP) and high (HP) phosphorus treatments. Growth stages are separated as panels A, seedling; B, budding; C, bolting; D, flowering; E, silique; F, ripening. Root length density is calculated based on the polycarbonate plate root traits. Values are mean±SE of 27 plants at the seedling stage and nine plants during the budding, bolting, flowering, silique and ripening stages. The vertical bar in the figures indicate the size of the least significant differences (LSD) to allow comparison of any two means each growth stage.

FIG. 5. Root dry weight (A), total plant dry weight (B), shoot dry weight (C) and root:shoot biomass ratio (D) of Zhongshuang 11 (*Brassica napus* L.) at different growth stages at low (LP) and high (HP) phosphorus treatments. Values are mean±SE of 27 plants at the seedling stage and nine plants during the budding, bolting, flowering, silique and ripening stages. The error bars indicate the standard error of the mean.

FIG. 6. P concentration in root (A), (mature) hypocotyl (B) and shoot (C, D) of *cv. Zhongshuang 11* (*Brassica napus* L.) during grown at low (LP) and high (HP) phosphorus treatments. Values are mean±SE of 27 plants at the seedling stage and nine plants during the budding, bolting, flowering, silique and ripening stages. The error bars indicate the standard error of the mean.

FIG. 7. Physiological P use efficiency (PPUE) of root (A), (mature) hypocotyl (B) and shoot (C, D) of *cv. Zhongshuang 11* (*Brassica napus* L.) grown at low (LP) and high (HP) phosphorus treatments. Values are mean±SE of 27 plants at the seedling stage and nine plants during the budding, bolting, flowering, silique and ripening stages. The error bars indicate the standard error of the mean.

$$\text{Physiological P use efficiency (PPUE)} = \frac{\text{Dry weight at HP } (DW_{HP})}{\text{Tissue P concentration at HP } (P_{high})} \text{ or } \frac{\text{Dry weight at LP } (DW_{LP})}{\text{Tissue P concentration at LP } (P_{low})}$$

Equation 1.

FIG. 1

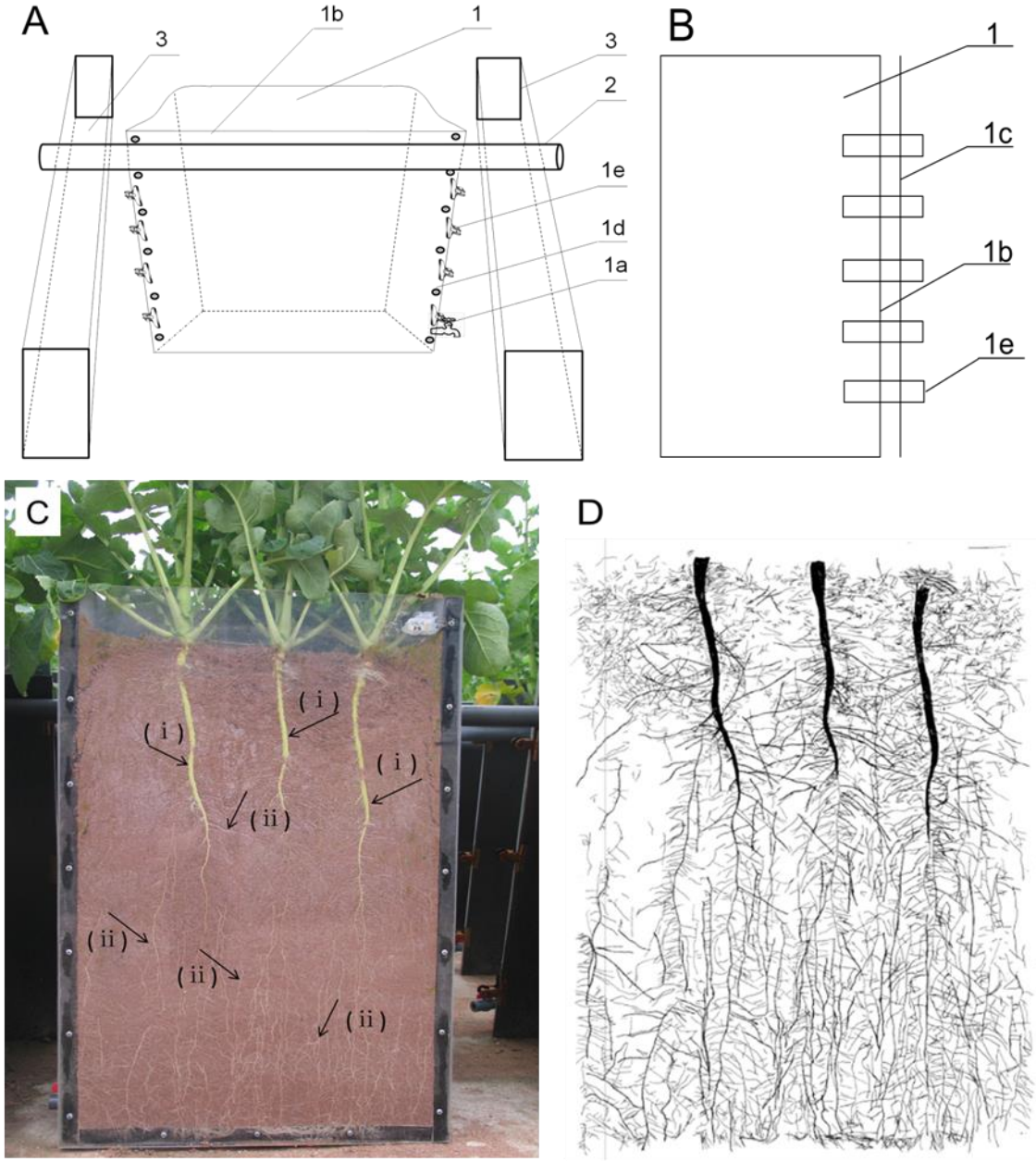

FIG. 2

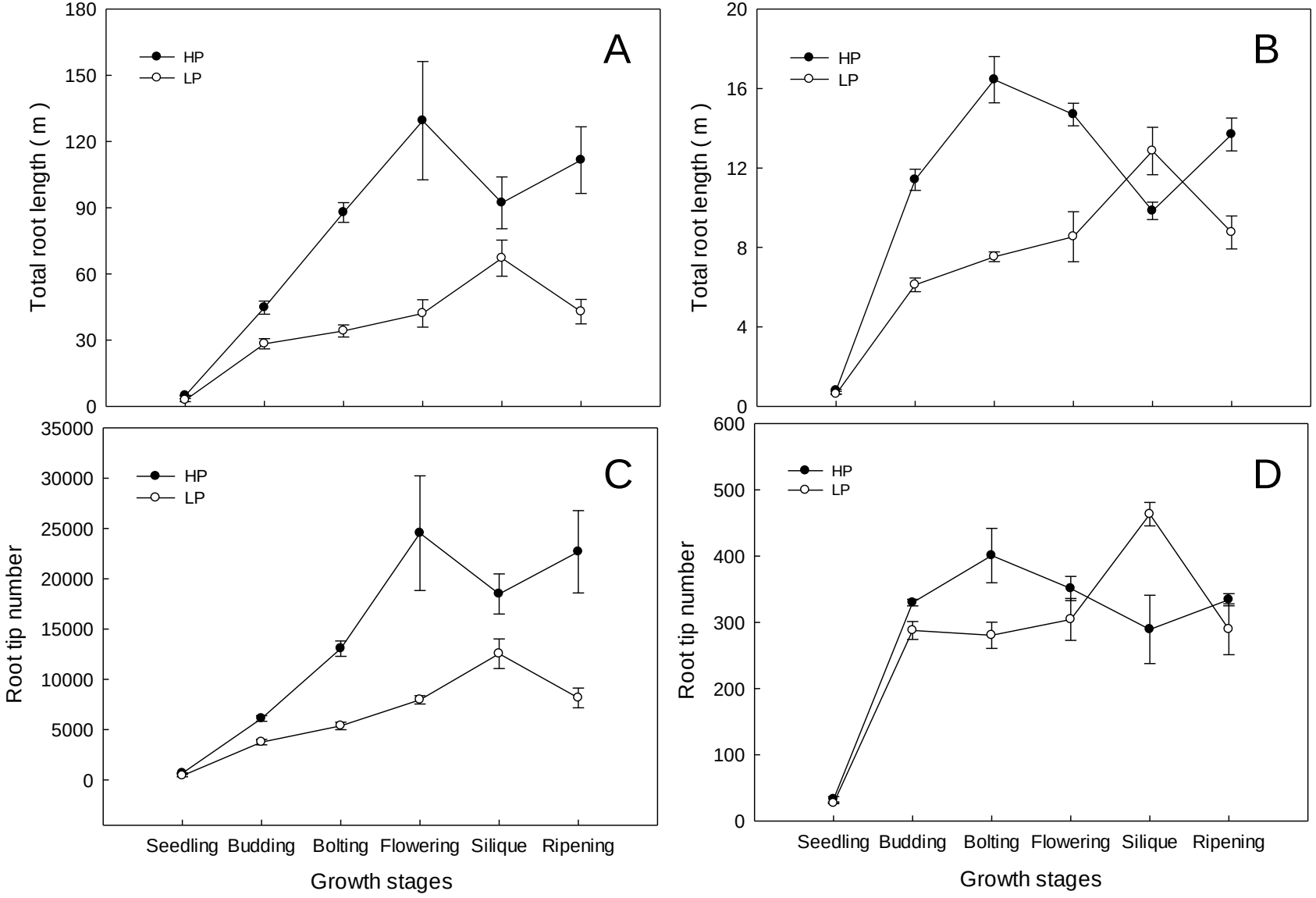
A
B
C
D
HP
LP
Total root length (m)
Root tip number
Seedling
Budding
Bolting
Flowering
Silique
Ripening
Growth stages

FIG. 3

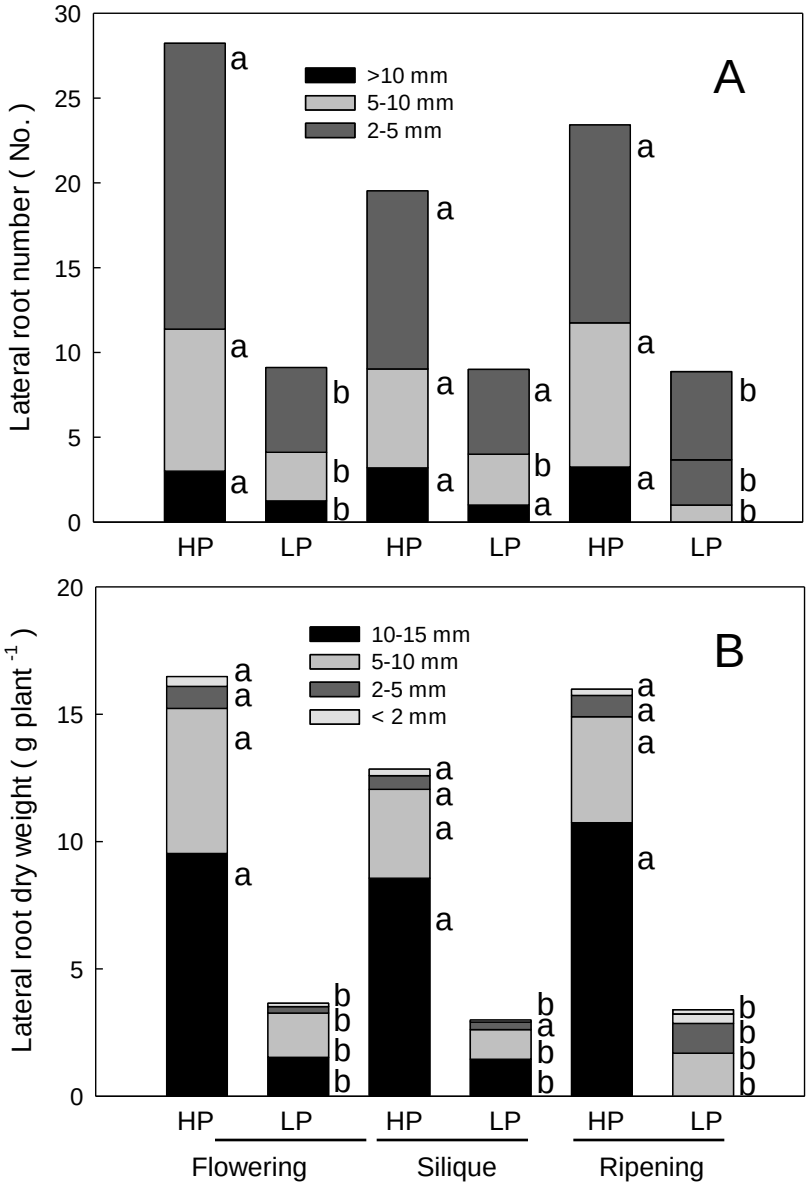
A
>10 mm
5-10 mm
2-5 mm
Lateral root number (No.)
30
25
20
15
10
5
0
HP
LP
B
10-15 mm
5-10 mm
2-5 mm
< 2 mm
Lateral root dry weight (g plant -1)
20
15
10
5
0
Flowering
Silique
Ripening

FIG. 4

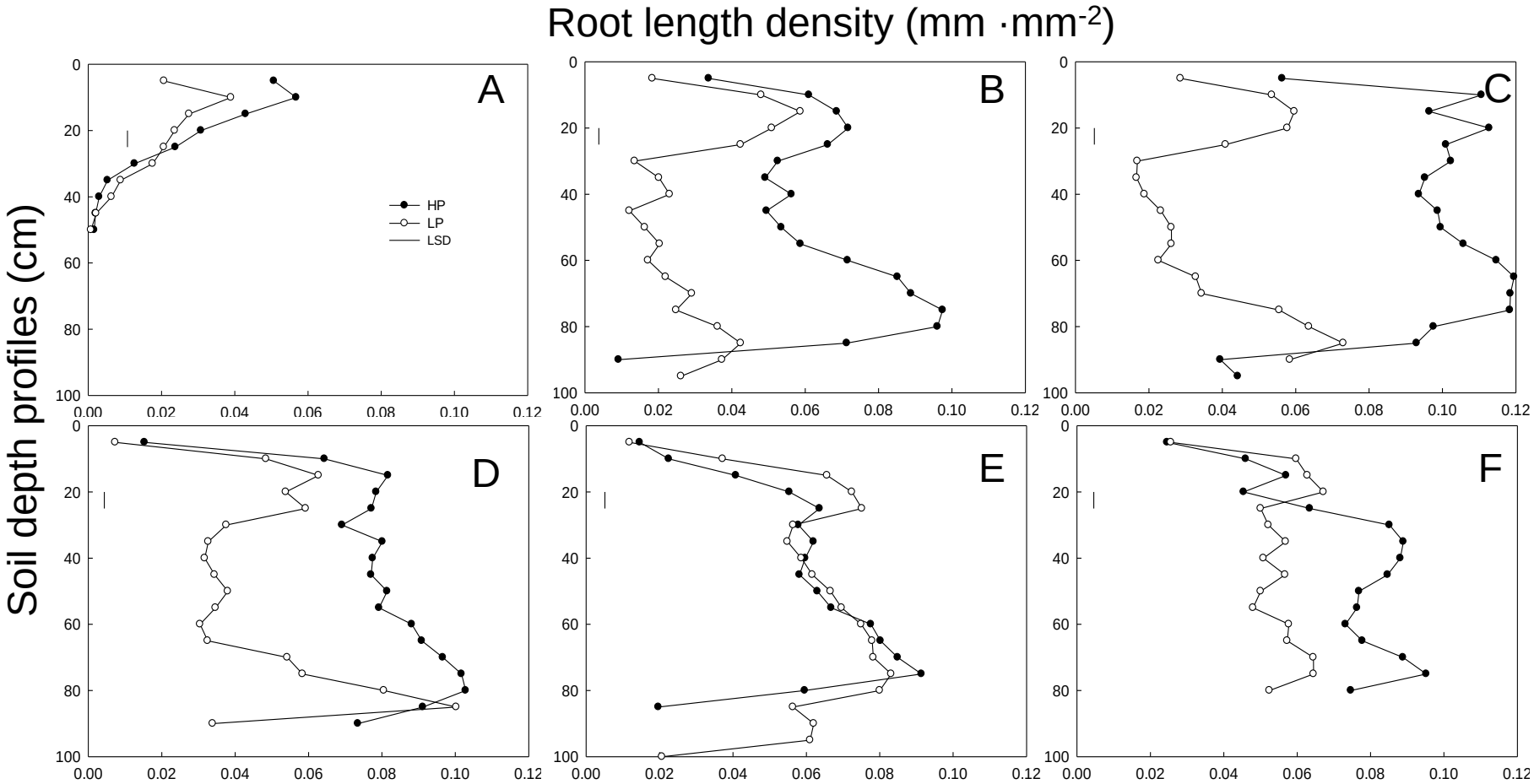
Root length density (mm ·mm-2)
Soil depth profiles (cm)
A
B
C
D
E
F
HP
LP
LSD
0
20
40
60
80
100
0.00
0.02
0.04
0.06
0.08
0.10
0.12

FIG. 5

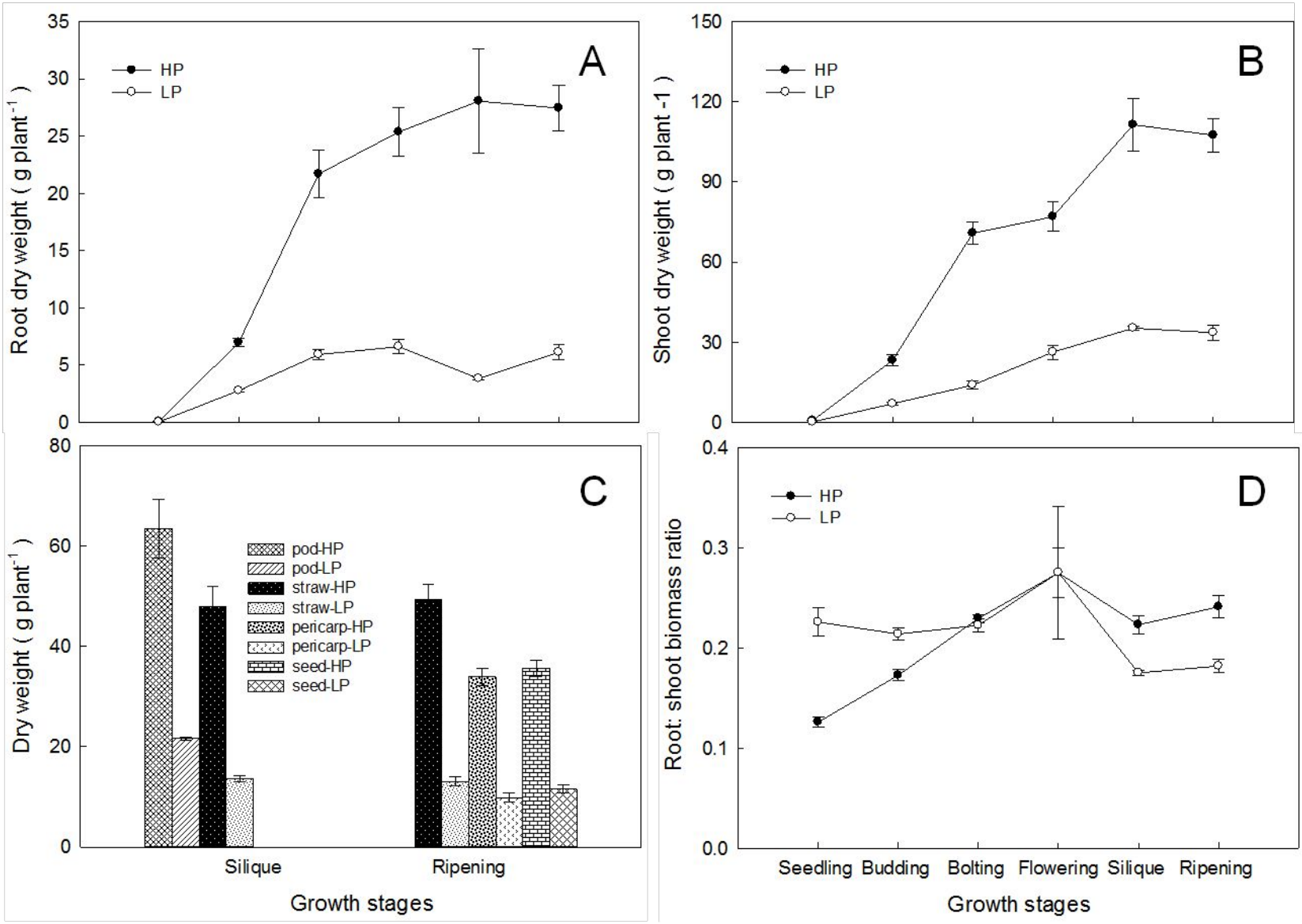
A
Root dry weight (g plant-1)
HP
LP
B
Shoot dry weight (g plant -1)
C
Dry weight (g plant-1)
pod-HP
pod-LP
straw-HP
straw-LP
pericarp-HP
pericarp-LP
seed-HP
seed-LP
Silique
Ripening
Growth stages
D
Root: shoot biomass ratio
Seedling
Budding
Bolting
Flowering
Silique
Ripening
Growth stages

FIG. 6

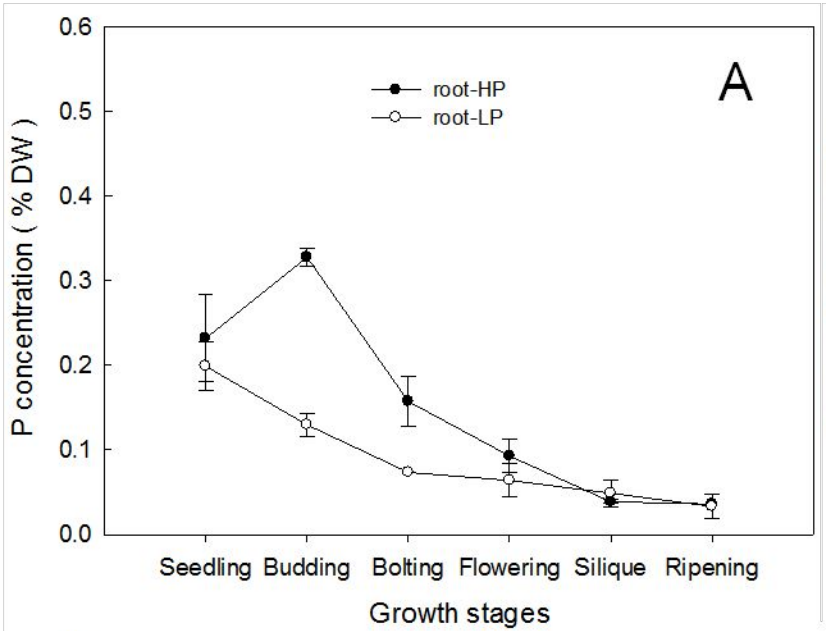
A
root-HP
root-LP
P concentration (% DW)
0.0
0.1
0.2
0.3
0.4
0.5
0.6
Seedling
Budding
Bolting
Flowering
Silique
Ripening
Growth stages

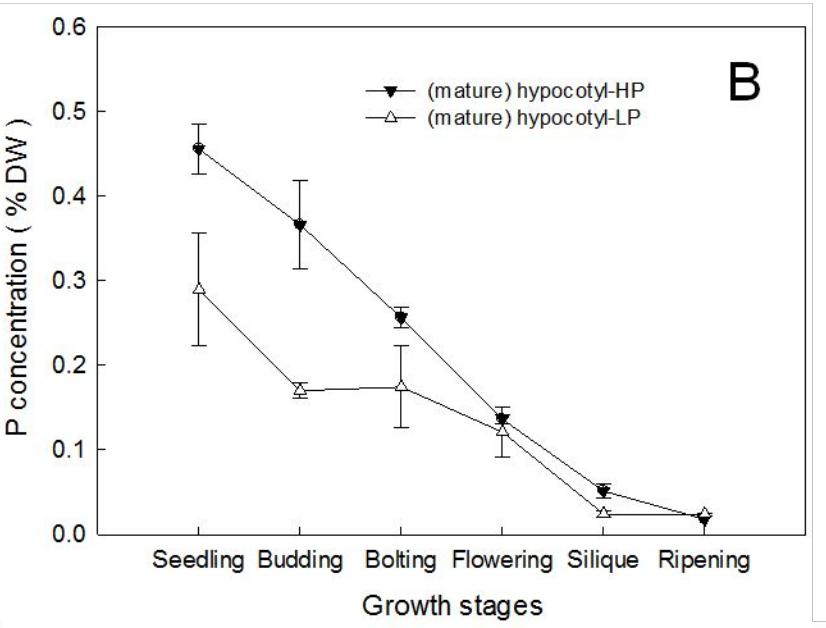
B
(mature) hypocotyl-HP
(mature) hypocotyl-LP
P concentration (% DW)
0.0
0.1
0.2
0.3
0.4
0.5
0.6
Seedling
Budding
Bolting
Flowering
Silique
Ripening
Growth stages

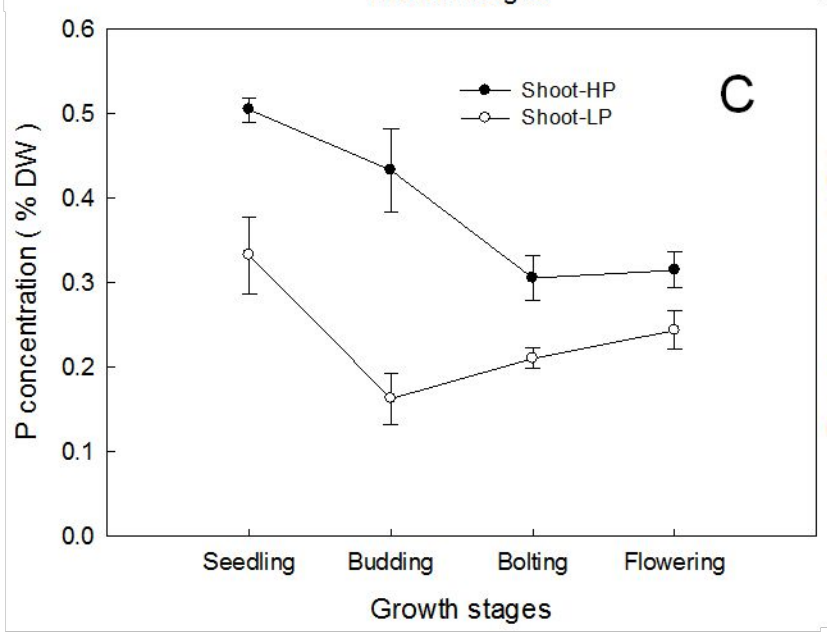
C
Shoot-HP
Shoot-LP
P concentration (% DW)
0.0
0.1
0.2
0.3
0.4
0.5
0.6
Seedling
Budding
Bolting
Flowering
Growth stages

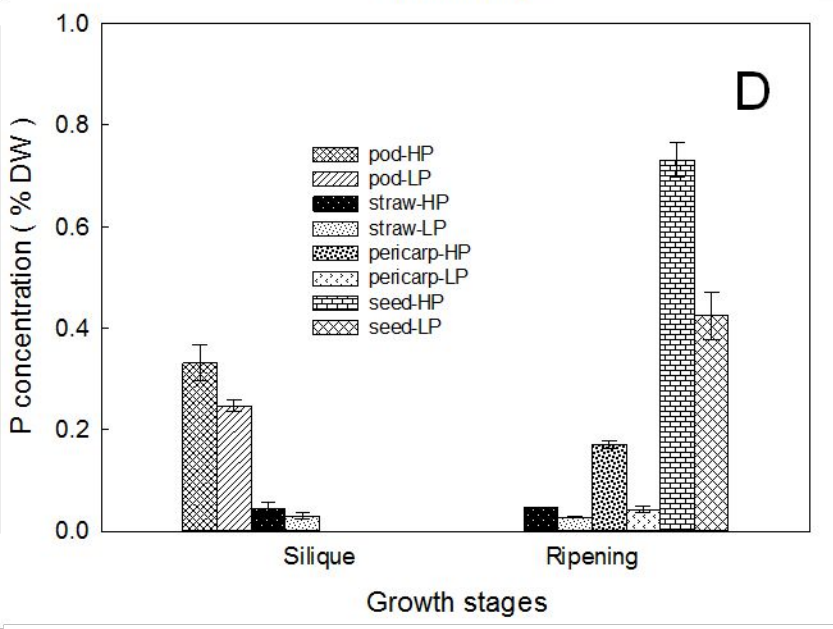
D
pod-HP
pod-LP
straw-HP
straw-LP
pericarp-HP
pericarp-LP
seed-HP
seed-LP
P concentration (% DW)
0.0
0.2
0.4
0.6
0.8
1.0
Silique
Ripening
Growth stages

FIG. 7

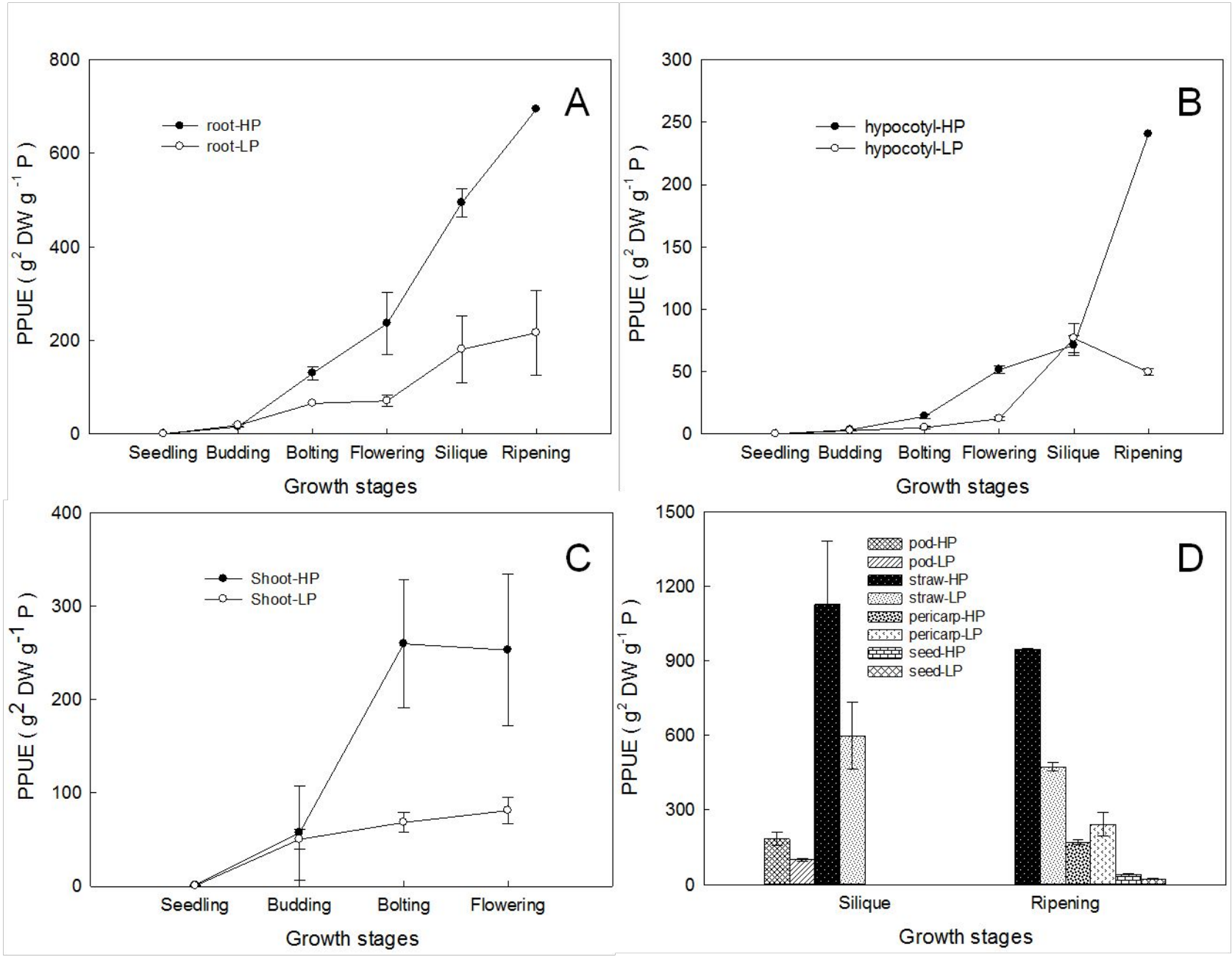
A
root-HP
root-LP
PPUE (g^2 DW g^{-1} P)
800
600
400
200
0
Seedling Budding Bolting Flowering Silique Ripening
Growth stages
B
hypocotyl-HP
hypocotyl-LP
PPUE (g^2 DW g^{-1} P)
300
250
200
150
100
50
0
Seedling Budding Bolting Flowering Silique Ripening
Growth stages
C
Shoot-HP
Shoot-LP
PPUE (g^2 DW g^{-1} P)
400
300
200
100
0
Seedling Budding Bolting Flowering
Growth stages
D
pod-HP
pod-LP
straw-HP
straw-LP
pericarp-HP
pericarp-LP
seed-HP
seed-LP
PPUE (g^2 DW g^{-1} P)
1500
1200
900
600
300
0
Silique Ripening
Growth stages